Journal of the Optical Society of Korea, Vol. 1, No. 2, September 1997, pp. 110-115

Cascaded Raman fiber amplifier operating at 1.3 μm using WDM couplers

Do Il Chang and Hong Jin Kong

Department of Physics, Korea Advanced Institute of Science and Technology
373-1 Kusong-Dong Yusong-Gu Taejon 305-701, KOREA

S.V. Chernikov, M.J. Guy, and J.R. Taylor

Femtosecond Optics Group, Imperial College, London SW7 2BZ, United Kingdom

(Received: July 7, 1997)

We report efficient cascaded Raman generation and signal amplification at 1.3 μm achieved in a ring resonator constructed solely from fiber components, i.e. fusion WDM couplers. Low-loss single-mode fiber with moderate GeO_2 content (18 mole %) is used as an active medium and pumped by a Nd:YAG laser at 1.064 μm. In a resonant cascaded geometry, this generates the third Stokes line at 1.24 μm, which acts as a pump for signal wavelength around 1.3 μm. A DFB laser operating at 1.315 μm is used to provide an input signal. An output signal powers up to 20 dBm (100 mW) with a 28 dB Raman gain are attained, where the Nd:YAG pump power is 3.4 W. It is also shown experimentally that it is important to use optical filters to suppress feedback from the resonator, permitting high Raman gain and good signal quality.

I. INTRODUCTION

The next generation of fiber optic communication systems will employ all-fiber amplifiers in the place of electronic repeaters. The principal advantage of an optical amplifier is its extremely wide gain band width ($> 10^{12}$ Hz) which makes it possible to amplify simultaneously a number of signals at different carrier wavelengths.

At present, fiber optic systems operate at the two communication windows of 1.5 μm and 1.3 μm, i.e. at the wavelengths of minimum optical losses and zero dispersion of standard silica-based fibers, respectively. A large amount of work has been done for both wavelengths concerning the use of fiber optic amplifiers [1] and it has been shown that 1.55 μm in conjunction with Erbium doped silica fiber gives a better and satisfactory property for the use of optical telecommunication system [2]. However, the vast majority of currently installed fiber optical communication systems in the world operate at 1.3 μm due to its earlier development and implementation. Therefore, the development of high gain optical amplifiers for the 1.3 μm communication window is of great interest.

To be compatible with existing systems, silica-based amplifiers are preferable, but there is currently no silica-based fiber amplifier which operates at 1.3 μm. The most promising contender for this wavelength is in fact not silica-based but fluoride-based (Praseodymium doped fluoride fiber amplifier; PDFFA) [3-8]. There are difficulties in using PDFFAs commercially, however, because they suffer from the disadvantages of difficulty in fusion splicing to normal silica transmission fiber, relatively high pump powers, low mechanical strength and high optical loss [3,4].

In this paper, we show that an efficient silica-based fiber amplifier at 1.3 μm can be realised through the use of Stimulated Raman Scattering (SRS). SRS-based amplifiers, also known as fiber Raman amplifiers [9] have received considerable interest for use in optical communication for both 1.55 μm [10-12] and 1.3 μm [13-18]. Although stimulated Raman scattering is a resonant effect, the bandwidth for light amplification in fiber is as wide as 200 cm^{-1} making this technique suitable for amplification of ultrashort pulses [19] or many WDM channels. Higher pump power requirements compared with Erbium amplifiers have generally precluded further development in the 1.5 μm spectral window. At 1.3 μm, however, the typical power requirement for a Raman amplifier is comparable to that for PDFFAs. Hence the Raman amplifier may be a competitive alternative if improved pumping schemes and more efficient amplifier configurations can be developed.

We demonstrate efficient cascaded Raman generation up to third Stokes order through a ring resonator configuration realised by using wavelength division multiplexer (WDM) fused fiber couplers. A CW

Nd:YAG laser at 1.064 μm is used to pump the system and high 1.315 μm signal amplification is achieved. This amplifier is based solely on standard silica fiber and a commercially available pumping system. It, therefore, is highly compatible with existing systems.

II. FIBER RAMAN AMPLIFIER

In the case of pure silicas, Raman gain is maximum for the frequency component that is down shifted from the pump frequency by about 13.2 THz (440 cm^{-1}). The most significant feature of silica fiber is that the Raman gain extends over a large frequency range (up to 40 THz) due to the non-crystalline nature of the silica glass. Pumping with a Nd:YAG laser at 1.064 μm, the process can cascade and several orders of Stokes emission are generated around 1.12, 1.18, 1.24, 1.31 and 1.38 μm, corresponding to Stokes shifts of 430, 458, 414, 434 and 390 cm^{-1}, respectively, and each successive Stokes line is broader than the preceding one [13]. For optimum performance of fiber Raman amplifiers employing silica fiber, the frequency difference between the pump and signal beams should correspond to the peak of the Raman gain. Therefore, the third order Stokes line at 1.24 μm can act as an efficient pump to amplify signals around 1.3 μm.

In the design of the Raman amplifier pumped at 1.064 μm, the idea is to create cascaded energy transfer to an optimised third Stokes order with the maximum efficiency. For this purpose, intracavity Raman generation is preferred in order to significantly decrease the SRS threshold and increase the efficiency of energy transfer from the pump to the Stokes orders [20,21]. At very high gain, however, a small amount of feedback around the fourth Stokes order can be enough to give rise to lasing around the signal wavelength, so care must be taken to suppress any unwanted feedback in the intracavity amplifier.

To separate different wavelengths generated by the SRS, either fiber Bragg gratings or fiber fusion WDM couplers can be used. Here we used a WDM configuration, because although fiber Bragg gratings are much easier to implement than the WDMs, the former only allows linear configurations while the latter allows reconfiguration to the ring resonator. Because the paths of signal and each Stokes order can be separated in the ring resonator configuration, it is easier to remove the small feedback of the signal wavelength, and better signal quality can be obtained. Also the WDM configuration has the advantage that counter propagating pump schemes, which are more efficient and preferable, can be readily implemented.

III. EXPERIMENTAL ARRANGEMENT

A schematic diagram of the experimental arrangement is shown in Fig. 1 The amplification system consists of two ring resonators (1.12,1.24 ring resonator and 1.18 ring resonator) formed by WDM fiber fusion couplers. A CW Nd:YAG laser at 1.064 μm is used as the pump source. The pump radiation is coupled into the fiber using 12.00 mm focal length, diode laser objective lens (T=94 % at 1060 nm, Newport, F-L10B), L. The Optical Faraday Isolator, OFI 1, to the pump laser is used to prevent feedback into the pump laser, which would cause instability. The signal source is a DFB laser (Lasertron, QLM1300DFB) operating at 1.315 μm. The fiber isolator, OFI 2, is used protect the DFB and ensure that the signal laser remained stable under all conditions. The pump and the input signal are combined into the fiber using WDM^{01}.

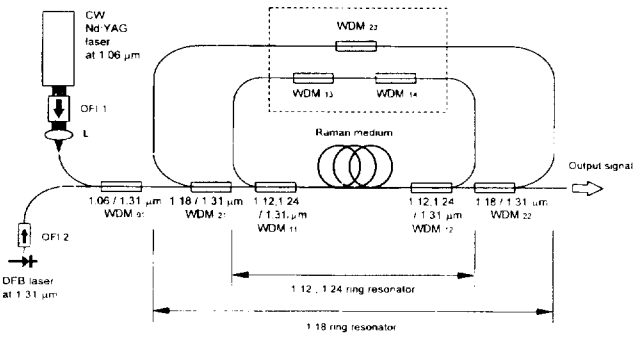

FIG. 1. Schematic diagram of the cascaded Raman amplifier; WDM, Wavelength Division Multiplexer; L, Objective Lens; OFR 1, OFR 2, Optical Faraday Isolator. Inside the dotted box ; Optical filters.

As an active Raman medium, low-loss single-mode fiber with moderate GeO_2 content (LYCOM, DK-SM) is used. The specification of the active fiber used in this experiment is in Table 1. The large difference between

TABLE 1. Specification of the active fiber (LYCOM, DK-SM)

Length		1,200 m
Δn		0.025
Mole%GeO_2 in core		18 %
Core diameter		2.32 μm
Cut-off wavelength		797 nm
Attenuation	1065 nm	1.83 dB/km
	1115 nm	1.52 dB/km
	1175 nm	1.23 dB/km
	1240 nm	1 dB/km
	1315 nm	0.78 dB/km
	1395 nm	0.84 dB/km
	1550 nm	0.38 dB/km
Model field diameter	1064 nm	3.19 μm
	1117 nm	3.39 μm
	1175 nm	3.60 μm
	1240 nm	3.86 μm
	1315 nm	4.18 μm
	1395 nm	4.62 μm
	1550 nm	5.59 μm

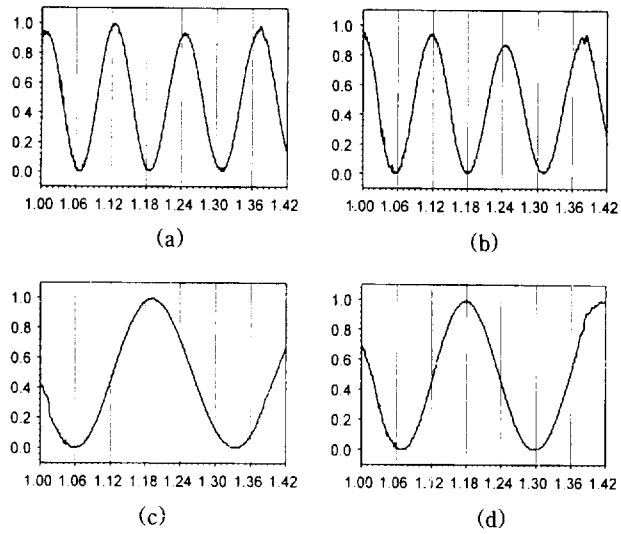

FIG. 2. Transmittance characteristics of the WDMs used as resonator couplers
(a) WDM_{11}, (b) WDM_{12} for the 1.12,1.24 ring resonator
(c) WDM_{21} (d) WDM_{22} for the 1.18 ring resonator
Horizontal axis; Wavelength (μm)
Vertical axis; Normalized transmittance
Transmittance is measured between two arms of WDM connecting ring resonator.

the refractive index of the core and cladding ($\Delta n = 0.025$) makes it possible to reduce the core diameter to less than 3 μm so that high pump power densities become feasible [22]. Moreover, the effective Raman gain coefficient has been found to depend linearly on the GeO_2 concentration, resulting in higher gain than would be possible with pure SiO_2 [23].

The fiber WDM couplers used are made by the fused biconical taper technique [24]. Low loss single-mode fiber (LYCOM, DSF) is used for the WDMs in this experiment. The fiber has a cut-off at 990 nm, a core diameter of 4.2 μm and the fiber loss is quite low, 0.39 dB/km at 1310 nm. To a good approximation, the wavelength response of a WDM coupler is sinusoidal and is described by;

$$T(\lambda) = \frac{1}{2}\left[1 + \sin\frac{2\pi}{\Delta\lambda}(\lambda - \lambda_q)\right] \qquad (1)$$

where $\Delta\lambda$ is the wavelength period of the coupler, $2\pi\lambda_q/\Delta\lambda$ is a phase parameter and $T(\lambda)$ is the transmission as a function of wavelength. Using a white light input source in conjunction with an optical spectrum analyser (Anritsu, MS9030A) with a resolution of 5 nm, transmittance characteristics of the WDMs are measured. These results for the resonator couplers are depicted in Fig. 2. In this Fig., the measured value of each WDM is normalized to make maximum transmittance to be unity. From the periodic characteristics of the WDM coupler, it can be seen that the transmittance of the WDM_{11} and WDM_{12} have maximum values near 1.12, 1.24, 1.38 μm and minima near 1.06, 1.18, 1.3 μm, between two arms connecting the ring resonator. Therefore, the first and third Stokes line generated by the active medium from the pump wavelength at 1.064 μm are resonated by WDM_{11}, WDM_{12} to form the 1.12,1.24 ring resonator (the inner loop in Fig. 1). Signal wavelength of 1.315 μm, second Stokes of 1.18 μm and pump wavelengths of 1.064 μm pass diverted through these WDMs. The couplers WDM_{21} ,WDM_{22} split off light at 1.18 μm, forming a resonator for the second Stokes line (the outer loop in Fig. 1).

The first Stokes is almost equally generated in both directions because the CW pump provides the same Raman gain for co- and counter propagation. Increasing the 1.064 μm pump above the threshold, the first Stokes order is quickly saturated, providing amplification for the next Stokes order at 1.18 μm. Being amplified inside the cavity the second Stokes exits through WDM_{11}, WDM_{12} and is resonated by WDM_{21}, and WDM_{22}. This resonator cavity simply provides the generation and storage of the second Stokes order to amplify the next Stokes at 1.24 μm in the gain medium. This third Stokes is again resonated and stored in the 1.12,1.24 ring resonator, similar to first Stokes.

IV. OPTIMIZATION OF THE AMPLIFIER BY ADDING OPTICAL FILTERS

Lasing around 1.3 μm (the fourth Stokes) is significantly suppressed in both resonators of the amplifier by the WDMs, each providing more than 30 dB peak isolation. However, these couplers have a periodic sinusoidal characteristic and Raman gain exhibits a very

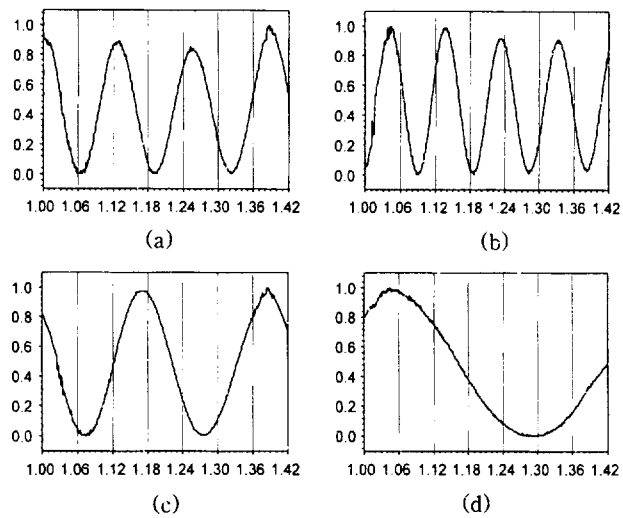

FIG. 3. Transmittance characteristics of the WDMs used as optical filters (a)-(c) and power coupler (d)
(a) WDM_{13} (b) WDM_{14} for the 1.12/1.24 ring resonator
(c) WDM_{23} for the 1.18 ring resonator (d) WDM_{01} power/signal coupler
Horizontal axis; Wavelength (μm),
Vertical axis; Normalized transmittance.

broad bandwidth. In the very high gain amplifier, the small amount of feedback around the minimum transmission wavelength of the WDM characteristics gives rise to lasing around 1.3 μm. Also, the periodic characteristics of the WDM_{11} and WDM_{12} can result in resonance of the fifth Stokes order near 1.38 μm. This acts as a loss mechanism at the signal wavelength, and so affects the efficiency of the signal amplification. To increase the wavelength discrimination and prevent fifth order generation, extra couplers(WDM_{13}, WDM_{14} for 1.12,1.24 ring resonator and WDM_{23} for 1.18 ring resonator) acting as optical filters are added to the configuration inside both resonators. Fig. 3. shows the normalized transmittance of the optical filters((a) - (c)) and power/signal coupler(d) and Fig. 4 shows the transmittance characteristics of the overall ring resonators which are combinations of several WDMs, in the absence(a) and in the presence(b) of the optical filters. The 1.12,1.24 ring resonator consists of two resonator couplers, WDM_{11}, WDM_{12} and two optical filters, WDM_{13} ,WDM_{14}. In this resonator, WDM_{13} which has similar characteristics to the 1.12,1.24 resonator couplers gives the sharp peaks of the first and third Stokes and reduces the possibility of feedback of the fourth Stokes wavelength. WDM_{14} which has the minimum transmittance near the wavelength of 1.38 μm suppresses the fifth Stokes generation. Without optical filters, the transmittance of the resonator is an additional maximum near 1.38 μm (Fig. 4, (a)), therefore, with a high power pumping, the fifth order Stokes may possibly be generated and can affect the amplification gain.

Since the second Stokes passes through WDM_{11} and WDM_{12}, they can give the sharp peak of the second Stokes line also, so the 1.18 ring resonator consists of two resonator couplers, WDM_{21}, WDM_{22} and three optical filters, WDM_{11}, WDM_{12} and WDM_{23}, In this resonator, WDM_{23} suppresses any feedback of the fourth Stokes wavelength and gives an additional sharp peak at the second Stokes.

In practice, the fabricated couplers do not have the exact sinusoidal characteristics. However, it is possible to simulate the performance of the resonator, which is the combination of multiple WDMs, by simply multiplying the normalised transmittance functions. Dotted curves in Fig. 4 show the simulation data for the transmittance in each case and it can be seen that the simulated estimation are in good agreement with the experimentally measured ones.

V. EXPERIMENTAL RESULTS AND DISCUSSION

Cascaded Raman spectra when pumped by Nd:YAG

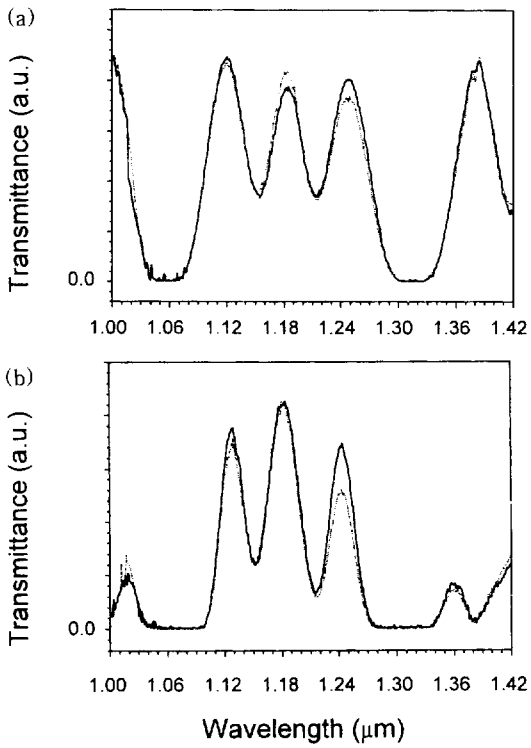

FIG. 4. Transmittance characteristics of the ring resonators
(a) in the absence of optical filters,
(b) in the presence of optical filters.
Solid line - measured data; Dotted line - calculated data.

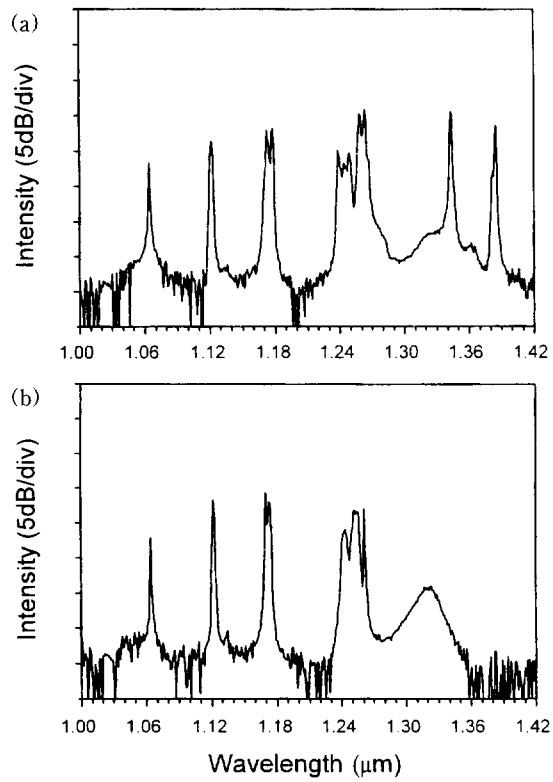

FIG. 5. Raman spectrum at output of amplifier without input signal
(a) in the absence of optical filters,
(b) in the presence of optical filters.

laser at 1.064 μm were observed at the output of the system using the optical spectrum analyser with 0.1 nm resolution. Typical spectra in the absence and in the presence of the optical filters are shown in Fig. 5(a), (b), respectively, where the pump power is 3W and no signal is applied. They have three similar Stokes lines with wavelengths around 1.12, 1.18 and 1.25 μm which coincide with the peaks of the transmittance of the amplifier in Fig. 4, but trace (a) displays additional peaks near the wavelengths of 1.34 and 1.38 μm. The first of these is probably due to the small feedback of the WDM resonator couplers and may deteriorate the amplified signal quality when the signal is applied. As expected, the periodic characteristics of the 1.12/1.24 ring resonator which has a peak around 1.38 μm generates the fifth Stokes. Trace (b) shows good suppression of the fourth and fifth order Stokes lines. In this case, the pump energy has been efficiently transferred to the third Stokes line at 1.25 μm, and this line is capable of providing gain to a signal near 1.3 μm.

The signal gain characteristics of the amplifier were investigated for the configuration including optical filters. Fig. 6 depicts the signal gain obtained for a range of launched pump powers. The input signal power during this measurement was $\sim$ 0.5 mW. The Raman gain is defined as the ratio of the amplified signal power to the signal output power without the pump light. In this case, it does not take into account the passive loss of the amplifier at 1.315 μm. The loss of the at 1.315 μm signal through the umpumped amplifier is merely the passive loss of the silica fiber and any WDM couplers and splice loss. In this experiment, it was measured to be about 5 dB but further optimization could reduce this value to be less than 2 dB. The pump power threshold for Raman amplification in this system is 1 W at 1.064 μm. The maximum Raman gain of 28 dB was achieved for 3.4 W pump power.

This maximum gain is expected to increase further with higher pump powers. The output spectrum from the amplifier in the presence of optical filters with an input signal is shown in Fig. 7. This graph indicates

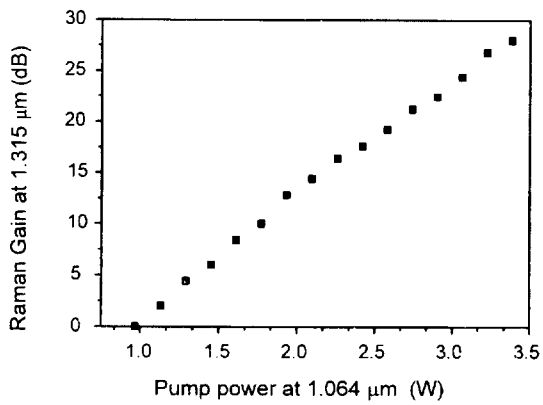

FIG. 6. Dependence of Raman gain at 1.315 μm on launched pump power.

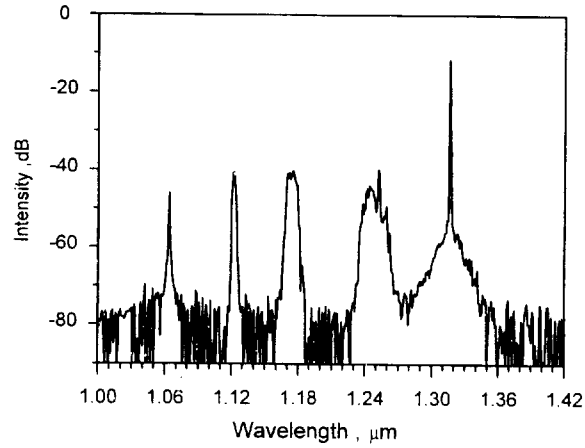

FIG. 7. Raman spectrum at output of amplifier with input signal.

the maximum output power from the amplifier was at the input signal wavelength of 1.315 μm with other wavelengths suppressed by $\sim$30 dB. The peak of the Raman gain of the fourth Stokes order coincides with the signal wavelength, and therefore, provides high amplification. It is noted that the power of the first to the third Stokes orders are nearly equal and well confined, indicating efficient Stokes generation and energy transfer from pump power to the higher Stokes orders. Fifth Stokes generation was not observed in this configuration even at the maximum pump power of 3.4 W. The input and output signal spectra are shown in Fig. 8, where the output signal power is 100 mW with 28 dB Raman gain. In the Raman amplifier, noise results from the spurious amplification by SRS of the spontaneous Raman light produced by the pump wave as it propagates along the fiber. The signal to noise figure(SNF) is obtained using the relationship [25].

$$\mathrm{SNF[dB]} = 10 \log \left(\frac{P_{spon}}{h\nu \cdot \Delta\nu \cdot (G-1)} \right) \qquad (2)$$

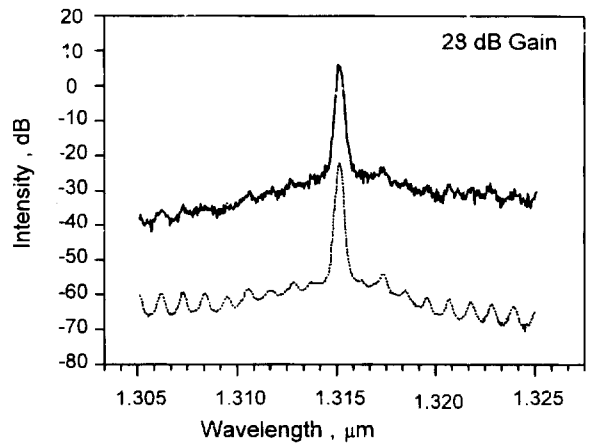

FIG. 8. Spectrum of amplified signal (solid line) and input signal (dashed line).

where P_{spon} is the amplified spontaneous Raman scattering power measured at bandwidth $\Delta\nu$, hν the energy of the photons, G the net gain factor. Depending on the stability of the large frame pump laser, which can now be replaced by stabilized diode pumped fiber lasers permitting better amplified signal quality, the noise figure measured lay in the range $4 \sim 6$ dB.

VI. CONCLUSIONS

We have investigated the characteristics of cascaded Raman amplification in a ring resonator configuration using fiber WDM couplers pumped at 1.064 μm with a Nd:YAG laser. In this experiment, a Raman gain of 28 dB with 100 mW output signal at 1.315 μm have been obtained. Efficient cascaded Raman generation up to third order Stokes has been achieved in the ring resonator configuration using fiber WDM couplers and optical filters. As a result, it is confirmed that the intracavity Raman resonator requires some optical filters to achieve high gain and improve amplified signal quality. Further improvement of the amplifier would be seen through optimizing the characteristics of WDM coupler/filters and reducing the splice loss through using the same fiber for the WDMs and active medium. The use of a diode-pumped ytterbium-doped fiber laser as the pump source is expected to yield not only spectacular improvements in the efficiency of the system, but also a reduction in the noise seen in the system. These measurements do, however, indicate that with optimized pumping source and employing simpler amplifier configurations, highly efficient, high gain, low noise amplifiers for the 1.3 μm window should be readily obtained. The cascaded Raman amplifier should also provide an efficient and effective means of expanding the usable bandwidth of existing and future optical transmission systems.

ACKNOWLEDGMENTS

Do Il Chang thanks the British Council for the support during the course of this research at the Imperial College in UK.

REFERENCES

[1] A. Bjarklev,"Optical fiber amplifiers: Design and System Applications", (Artech House Inc., 1993).

[2] E. Desurvire, "Erbium-doped fiber amplifiers: principles and applications", (John Wiley & Sons Inc., New York, 1994).

[3] S. T. Davey and P. W. France, Br. Telecom Technol. J. **7**, 58 (1989).

[4] R. Wyatt, T. Whitley, S. Davey and D. Szebesta, Proc. SPIE Int. Soc. Opt. Eng.**1789**, 170 (1992).

[5] T. J. Whitley, J. Lightwave Technol. **13**, 744 (1995).

[6] N. Tomita, K. Kimura, H. Suda, M. Shimizu, M. Yamada and Y. Ohishi, IEEE Photon. Technol. Lett. **6**, 258 (1994).

[7] M. Yamada, M Shimizu, H. Yoshinaga, K. Kikushima, T. Kanamori, Y. Ohishi, Y. Terunuma, K. Oikawa and S. Sudo, Electron. Lett.**31**, 806 (1995).

[8] S. Sanders, K. Dzurko, R. Parke, S. O'Brien, D.F. Welch, S.G. Grubb, G. Nykolak and P.C. Becker, Electron. Lett. **32**, 343 (1996).

[9] G. P. Agrawal, "Nonlinear fiber optics", (Academic Press, 1995) chapter 8.

[10] K. Nakamura, M. Kimura, S. Yoshida, T. Hidaka, and Y. Mitsuhashi, J. Lightwave Technol. **LT-2**, 379 (1984).

[11] M. Nakazawa, T. Nakashima and S. Seikai, J. Opt. Soc. Am. B. **2**, 515 (1985).

[12] L. F. Mollenauer, R. H. Stolen and M. N. Islam, Opt. Lett. **10**, 229 (1985).

[13] M. Nakazawa, M. Tokuda, Y. Negishi and N. Uchiba, J. Opt. Soc. Am B. **1**, 80 (1984).

[14] E. M. Dianov, D. G. Fursa, A. A. Abramov, M. I. Belovolvo, M. M. Bubnov, A. V. Shipulin, A. M. Prokhorov, G. G. Devyatykh, A. N. Gur'yanov and V. F. Khopin, Sov. J. Quantum Electron. **24**, 749 (1994).

[15] S. G. Grubb, T. Erdogan, V. Mizrahi, T. Strasser, W. Y. Cheung, W. A. Reed, P. J. Lemaire, A. E. Miller, S. G. Kosinski, G. Nykolak and P. C. Becker, Proc. ECOC' 94, paper PD3, (1994).

[16] S. V. Chernikov, Y. Zhu, R. Kashyap and J. R. Taylor, Electron. Lett. **31**, 472 (1995).

[17] E. M. Dianov, V. I. Karpov, M. V. Grekov, A. M. P'rokhorov, V. F. Kamalov and E. V. Slobodchikov, Electron. Lett. **32**, 1481 (1996).

[18] P. B. Hansen, A. J. Stentz, L. Eskilden, S. G. Grubb, T. A. Strasser and J. R. Pedrazzani, Electron, Lett. **32**, 2164 (1996).

[19] A. S. Gouvenia-Neto, A. S. L. Gomes, J. R. Taylor, B. J. Ainslie and S. P. Craig, Electron, Lett. **23**, 1034 (1987).

[20] Th. Lasser, H. Gross, W. Ulrich, P. Greve, and H. J. Niederwald, Proc. SPIE. Int. Soc. Opt. Eng. **1132**, 36 (1989).

[21] D. I. Chang, J. Y. Lee, and H. J. Kong, Appl. Opt.**36**, 1177 (1997).

[22] T. Nakashima, S. Seikai and M. Nakazawa, Opt. Lett.**10**, 1420 (1985).

[23] J. M. Gabriagues, Proc. SPIE Int. Soc. Opt. Eng . **1171**, 43 (1989).

[24] I. Andonovic and D. Uttamchandani, "Principles of modern optical systems", (Artech House Inc., 1989) chapter 9.

[25] G. Cancellieri, "Single-mode optical fiber measurement: characterization and sensing", (Artech House Inc., 1993) chapter 4.